Minimizing bacterial adhesion on membrane: Multiscale characterization of surface modifications

Abigail Burato Rosales, Nadège Durban-Benizio, Xuan Loc Nguyen, Vincent Bouvier, Clémentine Lamo, Irem Demir-Yilmaz, Christel Causserand, Cécile Formosa-Dague, Clémence Coetsier

Minimizing bacterial adhesion on membrane: multiscale characterization of surface modifications

Abigail Burato Rosales[a], Nadège Durban-Benizio[a], Xuan Loc Nguyen[a,d], Vincent Bouvier[a], Clémentine Lamo[a], Irem Demir-Yilmaz[b,c], Christel Causserand[a], Cécile Formosa-Dague[b,d*], Clémence Coetsier[a,d*]

[a] Laboratoire de Génie Chimique, Université de Toulouse, CNRS, INPT, UPS, Toulouse, France

[b] TBI, Université de Toulouse, INSA, INRAE, CNRS, 31000 Toulouse, France

[c] LAAS, Université de Toulouse, CNRS, Toulouse, France

[d] Fédération de Recherche Fermat, CNRS, Toulouse, France

Corresponding authors: Clémence Coetsier, clemence.coetsier@univ-tlse3.fr
Cécile Formosa-Dague, formosa@insa-toulouse.fr

Highlights

- Filtration at low frontal flux allows to optimize vanillin coating on PES membranes
- Homogeneous vanillin coating was confirmed by macroscopic and microscopic methods
- Single Cell Force Spectroscopy validates the reduction of bacterial adhesion forces
- AFM and EFM assess vanillin coating effect at different stages of biofilm growth
- PES-VAN membrane is efficient to reduce bacterial adhesion and EPS production

Abstract

The control of biofouling is required to improve membranes performances for water filtration. In this context, developing bioinspired approaches to modify membranes and give them antifouling properties is an interesting alternative. In this study, we elaborated new anti-biofouling membranes by coating them with vanillin, a natural bioactive molecule acting as a Quorum Sensing Inhibitor (QSI). First, the adsorption of vanillin by filtration was optimized to obtain homogeneous surface modifications. The modified membranes were then characterized in terms of physical-chemical properties: the results showed that they were more hydrophobic and exhibited a 14% decrease in pure water flux. Then, their anti-fouling properties were evaluated using complementary multiscale characterization methodologies; AFM single-cell experiments showed that vanillin adsorption had an effect on both the probability of bacterial cells to adhere to the surface, and on the force of adhesion. Direct EFM and SEM observation and adhesion assays further confirmed the effect of vanillin-modified membranes at the population-scale which showed a decrease in the bacterial coverage rate up to 50 %. Altogether, it confirms the multifunctionality of vanillin-coated membranes against biofouling: reduction of bacterial initial adhesion by changing the membranes surface properties and reduction of biofilm formation by quorum sensing inhibition.

Keywords

Microfiltration, anti-biofouling, surface modification, interfacial characterization, atomic force microscopy

1. Introduction

Because of their high efficiency for water pollution remediation and the high quality of the produced water, membrane processes are nowadays considered as improved technologies for sustainable management of water resources [1, 2]. However, some issues remain, such as membrane biofouling, which significantly hinders the development of these processes. Membrane biofouling occurs through the deposition and accumulation of microorganisms on membrane surfaces. Approaching the surface, various sequential mechanisms are identified: initial reversible adhesion controlled by van der Waals, electrostatic and hydrophobic interactions, production of exopolymeric substances (EPS) leading to the irreversible attachment of the bacteria and implying steric interaction, then the development of the biofilm to a mature state at the surface and inside the pores of the membrane [3-5]. It results in a significant loss of membrane performance (increase in the pressure drop, decrease in membrane permeability, and decline in product quality) [6]. For these reasons, biofouling is responsible for a large part of the operating costs associated with membrane processes, which include high-frequency cleaning cycles (use of chemicals, water, and energy for back-flush and cleaning in place) and, consequently, replacement of filtration units after premature ageing. PolyEtherSulfone (PES) membranes are widely used for microfiltration, ultrafiltration, or nanofiltration in wastewater treatment, water disinfection processes, and pretreatment prior to desalination mainly because of their resistance to cleaning solutions [7]. But even in this case, to control biofouling development on these membranes, extensive chemical cleaning steps are needed, which generate all the disadvantages previously mentioned and considerably shorten the lifetime of membrane modules [8, 9]. In this context, controlling bioadhesion and biofouling would stabilize the water flux and help improve cleaning protocols, thereby meeting industrial challenges to increase membranes' lifetime and develop more efficient filtration processes for water treatment.

Different strategies to control biofouling and improve membrane cleaning have been explored. While optimization of hydrodynamic conditions represents an important part of these strategies, membrane surface modifications are also investigated [5, 10]. These recent years, bioinspired membranes have attracted increasing interest to improve the performances of the separation processes they are involved in [11]. These membranes reproduce the properties (forms, functions, etc.) of biological systems to solve technological problems, and in this sense, they represent the next generation of filtration membranes for water treatment [11-15]. Among these biological functions, those that control material fouling represent an important target as they could significantly contribute to improving the performance of membranes and of water treatment plants in which they are involved [16]. For that, some membrane modification strategies considered are those that: (i) mimic biological structures, such as grafting of polymers containing zwitterionic moieties [17], coating of thin film polymer brushes [18, 19], and creating Sharklet patterns on the membrane surface [20-22] to prevent physical-chemical interactions, and/or (ii) mimic biological functions, such as grafting to or adding in the bulk material of membranes antibacterial or enzymatic molecules to inhibit and/or kill microorganisms [23]. However, while for antibacterial there is a high risk to develop bacterial resistance, enzymes are costly and unstable [14]. The contact-type antibiofouling effects are promising to limit the adhesion of bacteria to the surface but is limited to micro-organisms that come into contact with the surface [24] with a risk for the cell contents to be released into the treated water. Thus, membrane surface modifications combining a reduction of the bacterial adhesion and in the biofilm development in a single step, easy to process and using non-dangerous chemicals are required.

An alternative and promising approach is to inhibit Quorum Sensing (QS), which is a form of intercellular communication used by bacteria to coordinate biofilm formation [25]. Inhibiting QS is a way to reduce the production of bacterial exopolysaccharides (EPS) needed for biofilm formation and responsible for biofouling growth, without the issues associated with antibacterial or enzymes. These recent years, numerous QS inhibitors (QSI) have shown promising results [26-29] towards different bacterial species. In nature, plants produce phytochemicals, such as phenolic aldehydes, which act as antimicrobial agents against a wide range of microbial species [30]. In particular, vanillin, a phenolic aldehyde from vanilla bean extract and a known QSI, reduced the biofilm of *Aeromonas hydrophila* isolated from a biologically

fouled reverse osmosis (RO) membrane on polystyrene surface by up to 46.3% [31, 32]. It was also demonstrated that a solution of 2 mM of vanillin could interfere with QS by binding to the active site of PqsR which acts as a response regulator in the QS signaling molecule, reducing *Pseudomonas aeruginosa*'s twitching motility and virulence [33, 34]. In addition to these demonstrated effects, vanillin presents major advantages compared to other phenolic compounds used for their bactericidal effects: (i) it is recognized as safe by the FDA (Generally Recognized As Safe, GRAS status), (ii) it has a disruption effect on bacteria cell wall probably due to its low intrinsic hydrophobicity and homeostatic effects [35], and (iii) it exhibits a bacteriostatic effect rather than a bactericidal one at measured inhibitory concentrations (MIC), preventing the establishment of bioresistance mechanisms [36]. Moreover, vanillin has recently been shown to inhibit biofilm formation in different bacterial species [37], while the use of other QSI may be species-dependent [38].Lastly, it was also demonstrated that vanillin could cause changes in the amount and composition of EPS produced by bacteria, which has consequences on the formation of biofilms and their structure [31, 37, 39-41]. Because of the multifunctional effects of vanillin, it is a promising candidate to be incorporated into a membrane material or grafted at a membrane surface to improve biofouling control. However, these multifunctional effects should be investigated further.

There are already studies exploring the effects of vanillin-modified membranes against different species. However, these studies are mainly focused on bacterial growth inhibition or on the changes it caused on the hydrophilicity or roughness of the materials, and there seems to be contradicting results when it comes to vanillin quantity, hydrophilicity, and membrane performance [42-45]. For instance, Esmaeili *et al.* showed an increase in polyethylene glycol (PEG) solution permeability after vanillin adsorption [42], but the correlation of permeability with hydrophilicity and vanillin adsorption on the membrane surface at high concentration of vanillin (>1.8 $g.L^{-1}$) was not clearly demonstrated. The authors thus suggested that the physical changes of the membrane surface could be responsible for the modification of the filtration performances. In another study, Shin *et al.* found a decrease of the water contact angle (WCA) on thin-film composite (TFC) RO membrane coated with vanillin (28°) compared to pristine membranes (40°), and there was minimal decrease in the surface roughness [43]. Despite the improvement in hydrophilicity, a 10% decrease in pure water permeability after the modification was reported. Nonetheless, they confirmed the inhibition of bacterial growth on the vanillin-coated membrane for *Escherichia coli* and *Bacillus subtilis* after 24 h of cultivation. However, no investigation was performed to observe the initial stage of bacterial adhesion. Lastly, Kumar *et al.* worked on the incorporation of vanillin by blending it into PES-based polymers [45]. When compared to virgin PES membranes, vanillin-modified membranes showed a higher permeability caused by an increase in the hydrophilicity and higher pore radius and volume due to thermodynamic instability. It also resulted in a bacteriostatic effect towards *E. coli* and *P. aeruginosa*. Although these studies illustrate new possibilities that the incorporation of vanillin, as a bioinspired approach, may offer to control membrane biofouling, further studies are needed to correlate the change of surface properties caused by vanillin and membrane performance. There are several hypotheses that could explain the anti-biofilm effect of vanillin membranes. It may be due to (i) the modification of the physical-chemical properties of the membrane by vanillin, or (ii) the biological properties of QS inhibition of vanillin, or (iii) a combined effect (additive or synergistic) of both. These could affect biofilm development at different stages, from initial adhesion to biofilm maturation (EPS production). While existing studies have focused on bacterial growth on modified membranes, so far, no work has investigated the effect of vanillin incorporation in membranes at different stages from initial bacterial adhesion/attachment to biofilm development. Moreover, the biofouling assessment techniques used for vanillin-modified membranes were indirect methods. Given the high sensitivity of biofilm formation to its environment, it is more appropriate to use direct observation of the biofouling evolution without introducing multiple environmental changes.

In this study, we modified with vanillin the surface of microfiltration membranes used for water treatment in reuse applications. For that, vanillin was adsorbed on PES membrane surfaces by filtration in optimized condition to increase the load rate and homogeneity of the surface coverage. Using these membrane samples, we then used, for the first time, a combination of direct and indirect techniques for surface characterization and imaging techniques at different size scales from macro- (contact angle measurement, FTIR mapping) to nanoscale (atomic force, epifluorescence, and electron microscopy) to further investigate and correlate the effects of vanillin on the membranes' physical-chemical properties, pure water flux, and initial bacterial attachment and biofilm maturation. Particularly interested in the first stage of adhesion, a new protocol was developed and assessed to directly evaluate bacterial adhesion at the population scale and coupled with measurements at single-cell level using AFM. This original approach provides a better understanding of the mechanisms responsible for the control of biofouling from a bioinspired approach using a natural biochemical molecule.

2. Experimental

2.1. Chemicals and Materials

Chemicals

Vanillin (99% reagent grade) was purchased from Alfa Aesar (UK). Phosphate-buffered saline solution (PBS 1X) was obtained from the dilution of a 10X stock solution provided by ThermoFisher. Culture media were prepared from powders: Tryptic Soy Broth (Corning), and Tryptic Soy Agar (VWR chemicals).

Fluorescent probes, SYBR™ Green I nucleic acid gel stain (10000X in DMSO), and Concanavalin A tetramethyl rhodamine conjugate, were provided by Invitrogen Thermofisher Scientific.

The solvents used in this work, methanol (HPLC grade), ethanol absolute (analytical grade), formaldehyde solution (38% in water), and hexamethyldisilazane (reagent grade, ≥99%), were purchased from Sigma-Aldrich Merck (FR). Hydrochloric acid 37% was from Acros Organics.

The commercial membrane used as support for this study was polyethersulfone (PES) membrane with a pore size of 0.04 µm, MicroPES® 1F PH. It was provided by Membrana GmbH (3M, Germany, Wuppertal).

Bacterial strains and growth conditions

Pseudomonas aeruginosa (PAO1, CIP104116) was purchased from the Centre de Ressources Biologiques de l'Institut Pasteur (France) as a freeze-dried sample. A single colony from Tryptic Soy Agar (TSA) was inoculated in 50 mL of Tryptic Soy Broth (TSB). After cultivation in TSB medium for 24h at 37°C, glycerol 20% final concentration was added to the culture. The mixture was divided into 1 mL aliquots that were stored at –20°C until their preparation for the experiments. Before the experimentation, 100 µL of *P. aeruginosa* cells from aliquot were cultured in TSB, 37°C, 150 rpm for 15h. Cells were then harvested by centrifugation (4100 g, 10 min, 6°C, JOUAN-G4-11) and rinsed in PBS 1X twice.

2.2. PES membranes coating with vanillin and evaluation of membrane filtration performances

Surface modification of PES membrane with vanillin via coating

PES membrane modification was obtained by filtration of vanillin through the PES membrane; the resulting membranes samples were called PES-VAN. As a control, membranes were also conditioned with only the solvent, PBS 1X pH=3.8, and were called PES-PBS. For that, PES membranes were cut into 44 mm diameter pieces and rinsed multiple times in hot MilliQ water (<60°C) to remove the preservative

agents. Membrane pieces were placed in a dead-end Amicon® filtration cell (Series 8050, Merck Millipore) with a backing fibrous layer with high porosity to avoid alteration of the membrane surface during filtration. The effective membrane surface is 13.4 cm² according to commercial specifications.

Pure water permeability was measured after a membrane compaction step at 0.6 bar for one hour (necessary duration to reach a stable permeate flux) and served as the ultimate washing of the membrane before the coating step. Filtration methods will be elaborated further in a section below.

Vanillin solution of 2000 mL at 3 $g.L^{-1}$ in PBS 1X, pH adjusted to 3.8, was filtered in this system at different transmembrane pressures, from 0.05 to 0.4 bar. The pH adjustment allows the vanillin to be in its protonated form (pKa 7.4) to avoid repulsive interaction with the negatively charged PES membrane [46]. After coating, PES-VAN membranes were rinsed with PBS 1X pH 3.8 to remove non-adsorbed vanillin from the surface and were then cut into several small pieces for the different characterization experiments.

Vanillin stability on the membrane was evaluated in two ways. The first evaluation was desorption under stirring wherein the PES-VAN membrane samples were immersed in ultrapure water and agitated at 150 rpm. The second assessment was through dead-end filtration at 0.1 bar wherein ultrapure water was filtered through the membranes. The desorption tests were done in triplicates for similar time (three hours) and water volume (2000 mL).

Coating quantity

The coating quantity of vanillin was obtained after extraction of the adsorbed vanillin from two or three pieces of the same membrane ($n \geq 3$) in an ultrasonic methanol bath. Based on a protocol described in the literature [47], this step was repeated three times. UV spectrophotometer (Lambda 365 Perkin Elmer) quantified the vanillin concentration in methanol according to a specific calibration curve. The coating quantity was calculated as the mean of membrane samples after summing the concentration of vanillin in methanol after three runs of extraction for each membrane sample.

Filtration experiments

Pure water flux, J, was assessed before and after the surface modification of the compacted PES membrane using equation 1 and the same filtration set-up as the one used for the PES membrane coating with vanillin.

$$J = \frac{Permeate\ volume\ (L)}{Effective\ membrane\ area\ (m^2) \times Time\ (h)} \qquad (1)$$

To assess the change in membrane filtration performance, pure water permeability, L_p, (equation 2) and flux decline ratio (FDR) (equation 3) were then calculated from the fluxes. J_o and J_f are the pure water fluxes before and after the membrane coating, respectively. FDR represents the flux decline after the modification step.

$$L_p = \frac{J}{\Delta P} \qquad (2)$$

$$FDR = \frac{J_f}{J_o} \qquad (3)$$

2.3. Characterization

Water contact angle measurements

Water contact angles (WCA) of membranes modified at different coating conditions were measured using the sessile drop method (Drop Shape Analyzer DSA30, KRÜSS, Germany). The results showed how the hydrophilicity changed upon modification of the membrane surface. 10 to 15 measurements were performed for each sample at different locations to reduce the experimental error. Average values were reported.

FTIR and IR mapping

Fourier transform infrared (FTIR) mapping of virgin and modified membranes was performed to determine the minimum quantity necessary to obtain a homogeneous coverage of the vanillin on the membrane surface, as described elsewhere [48]. Briefly, a Micro-FTIR spectrometer (iN10MX Thermo Fisher Scientific Nicolet) equipped with a liquid nitrogen-cooled MCT detector was used in ATR mode to scan 1.25 x 1.25 mm for each sample, meaning 6.25 mm² membrane surface for 4 samples in a row. One spectrum was registered for each 50x50 µm point (one point was measured every 50 or 100 µm) with a spectral resolution of 8 cm^{-1} for 16 scans. To generate the chemical maps, first, the absorbance peak unique to vanillin was identified, which is 1511 cm^{-1}, corresponding to the aromatic ring [49]. Then, the peak height was measured by taking the baseline limit. The chemical maps generated were color-coded according to the absorption peak height intensity with a rainbow color scale from blue (lowest intensity) to red (highest intensity). A higher peak intensity indicates more vanillin is present on the surface. The generated FTIR maps were not processed further except for the atmospheric correction. This technique visualizes the coating coverage on the surface but does not provide quantitative data. Thus, a python code was developed, as described elsewhere [50], to convert the colors on the chemical maps to peak height intensity average and standard deviation values. To summarize, first, the code transforms the image having a rainbow scale to a grey scale, from black (lowest intensity) to white (highest intensity). Then, using the grey values obtained from the image, it calculates the peak height intensity average value and standard deviation.

Attenuated total reflectance FTIR spectroscopy (ATR-FTIR) was used to validate the presence and relative quantity of vanillin on the PES membrane surface modified at different coating conditions. Average ATR-FTIR spectra were obtained from 3 independent measurements using ThermoNicolet 6700 spectrometer with Diamond ATR equipped with a DTGS detector. The spectral resolution was 4 cm^{-1}, and 16 scans were taken between 400 and 4000 cm^{-1}. The ratio of the absorbance of vanillin's specific peak at 1510 cm^{-1} (aromatic ring) to the PES's specific peak at 1485 cm^{-1} (aromatic band) was calculated to estimate the relative quantity of vanillin at different coating conditions.

AFM imaging, surface roughness, and apparent pore size estimation

Surface topography images of PES-PBS or PES-VAN membranes were recorded using atomic force microscope, AFM Nanowizard III (Bruker, USA), in contact mode in PBS 1X pH 7.4 at room temperature, using MLCT cantilevers (Bruker, USA, nominal spring constant of ~0.01 N/m, determined using the thermal noise method [51]) with a scanning rate of 4 Hz and a resolution of 512 x 512 lines. Roughness measurements (Ra) were performed using JPK Data Processing software (Bruker, USA) on 5 areas of 0.5 x 0.5 µm at the surface of the membranes. The apparent pore size was calculated using two 10x10 µm AFM images of each sample. For each image, 15 pore size measurements were performed with standard image analysis procedures using ImageJ. Lastly, the mean and standard deviation were calculated.

2.4. Bacterial adhesion and antifouling properties evaluation

Adhesion test and microscopic observations

The effect of vanillin on the adherence of *P. aeruginosa* (*Pa*) to the PES membrane surface was studied by performing culture tests in microplates. Several tests with the control membranes, PES-PBS, were performed to validate the conditions under which the adhesion tests will be carried out, with the objective to reduce the disturbances that may result from agitation and sedimentation conditions. Indeed, agitation of the medium can generate stress and stimulate the production of EPS which will hinder the counting and estimation of the number of cells adhered to the surface of the membrane [52]. Furthermore, if the membrane is placed at the bottom of the culture well, in the absence of agitation, the deposition of DNA and cell fragments by sedimentation can lead to a bias in the estimation of the initial adhesion of cells to the PES membrane surface [53]. To counteract the sedimentation phenomena, inserts (CellCrown, Scaffdex) were used to keep the membrane coupon immersed upside down in the medium on the top of

the culture well (Figure 1). Thus, only mass transport mechanisms governed by convection and diffusion are responsible for bacterial colonization and adhesion in our experiments.

Bacteria adhesion tests (biotic condition) with and without inserts, under agitation at 150 rpm and without agitation, were first performed on triplicate PES-PBS membrane samples (1.5 cm^2) in a 12-well culture plate. Once the optimum conditions were identified, bacterial adhesion tests were then performed on PES-VAN membranes. As a control, triplicates of PES-PBS and PES-VAN membrane samples were also introduced in sterile 12-well culture plates under abiotic conditions.

For abiotic condition tests, 2 mL of sterile PBS 1X at pH 7.4 was added to each well. This pH was chosen as the physiological pH for bacterial assays. For the biotic condition, 2 mL of *Pa* resuspended in PBS 1X (pH 7.4) at a cell concentration of about 10^7 $CFU.mL^{-1}$ was added to the corresponding well. Lastly, the plates were incubated at 37°C for 3h in the dark.

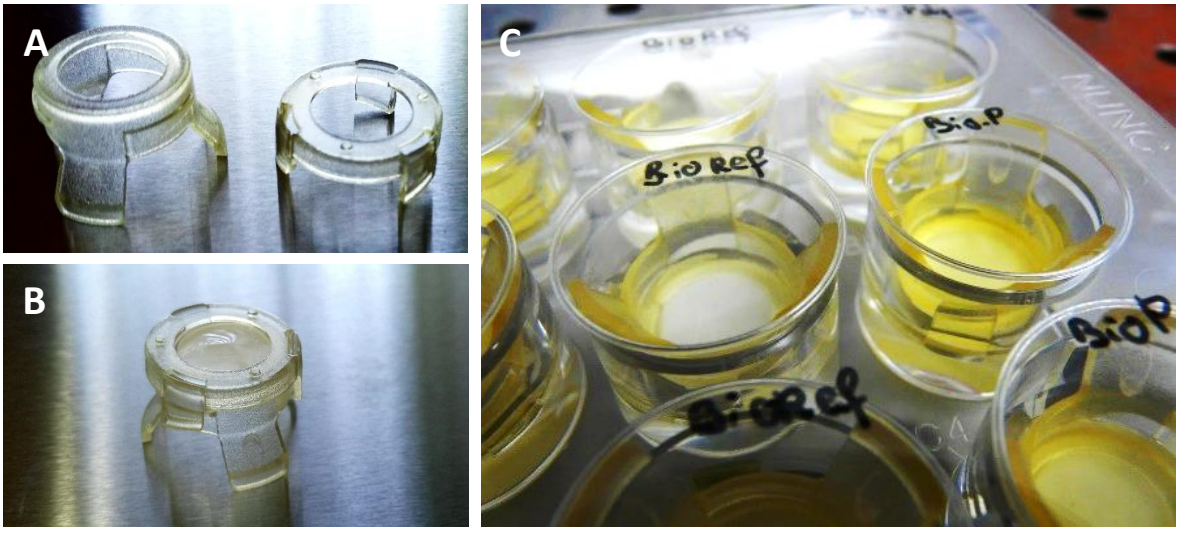

Figure 1. *CellCrown inserts to support the membrane during adhesion experiments. (A) Opened insert, (B) Insert with membrane, (C) Inserts in a 12-well culture plate.*

EFM imaging

The bacteria adhered to the membrane surface were directly observed under an epifluorescence microscope (EFM) after specific staining. The membrane samples were carefully rinsed three times with 1 mL of PBS 1X (pH = 7.4; ThermoFisher) to remove the bacteria not adhered to the surface. For the labeling step, the samples were completely immersed for 15 min in a solution of PBS 1X and SYBR™ Green (Invitrogen, USA) with a final stain concentration of 10X. The staining solution was then gently removed, and the samples were rinsed with PBS 1X to remove the excess stain before microscopic observations.

The calculation of the coverage rate by *Pa* was carried out with the Zeiss Zen Blue software on three independent membrane samples taking 40 to 50 images on each sample to obtain a satisfactory statistical representation of the observed phenomenon. A Z-stack acquisition (10 in-depth scans) was performed at 20x magnification. The Extended Depth of Focus tool was used to reconstruct a planar image when necessary. The bacteria were quantified by defining a circular area with a diameter of 216 µm to eliminate the non-homogeneous fluorescence between the center and the edge of the image.

SEM imaging

To further verify the structuration of the biofilm on PES-PBS and PES-VAN membranes, images were taken using a scanning electron microscope (SEM-FEG Jeol JSM 7100F-TTLS Tokyo, Japan) at 10 kV. Before performing SEM observations on biological samples, it is essential to have a good sample preparation protocol. For this purpose, the protocol described by Voegel *et al.* [54] was adapted to the membrane samples. They were immersed in a solution of 4% paraformaldehyde (1:2), PBS 1X (1:4), and ultrapure water (1:4) for 1h at room temperature, as a fixation step. Then, they were washed twice with PBS 1X and 0.4 M sucrose (1:2) solution. Lastly, in consecutive order, the samples were gradually dehydrated in ethanol-water solution (50%, 70%, 90% of ethanol for 5 min each), pure ethanol (30 min), ethanol – hexamethyldisilazane (HMDS) solution (50%, 75% of HMDS for 15 min each), and pure HMDS (until total evaporation). Afterwards, a 60 s metallization with gold was immediately performed.

AFM Single-Cell Force Spectroscopy experiments

Cell probes were prepared using the protocol described by Beaussart *et al.* [55]. Briefly, colloidal probes were obtained by attaching a single silica microsphere (5 µm diameter, Bangs Laboratories) with a thin layer of UV-curable glue (NOA 63, Norland Edmund Optics) on triangular tipless cantilevers (NP-O10, Bruker, USA) and using a Nanowizard III AFM (Bruker, USA). The cantilevers were then immersed for 1 h in PBS 1X containing 4 mg/mL of dopamine hydrochloride (Sigma-Aldrich), rinsed in PBS 1X, and used directly for cell probe preparation. The cantilever spring constant was determined prior to cell immobilization using the thermal noise method [51]. To attach the bacterial cell, the colloidal probe was then brought into contact with an isolated bacterium and retracted. Proper attachment of the cell on the colloidal probe was checked using optical microscopy. These cell probes were used to measure the interactions between cells and PES-PBS or PES-VAN membranes at room temperature, using a maximum applied force of 0.25 nN, a constant approach retraction speed of 2.0 µm/s, and a contact time of 1 s, on areas of 1 x 1 µm. Data were analyzed using the Data Processing software from JPK Instruments (Bruker, USA). Adhesion forces histograms were obtained by measuring the height of the biggest peak in each retract curves for each force curve. For each condition, experiments were repeated for 7 bacteria coming from 3 independent cultures.

AFM quantification of the membrane hydrophobicity

To measure the membrane's surface hydrophobicity, a recently developed method was used [56] which consists in measuring, using Fluidic force microscopy (FluidFM), the interactions between a bubble (hydrophobic interface in water) and the membranes. For that, FluidFM probes with an aperture of 8 µm in diameter (Cytosurge AG, Switzerland) were hydrophobized by coating with self-assembled monolayers (SAMs) of silanes *via* SAMs vapor deposition technique. FluidFM cantilevers were functionalized with 1H,1H,2H,2H-Perfluorodecyltrichlorosilane (FDTS) using Orbis-1000 equipment (Memsstar, Livingston, UK) to make their external surface and inside microchannel hydrophobic. The deposition was realized under vacuum at 0.05 bar and -40°C, for 5 min. Then, the microchannel of these silanized cantilevers was filled with air and the probe was immersed in PBS 1X. To eliminate any particle or dust contamination or to prevent clogging of the FluidFM cantilever, a slight overpressure of 20 mbar was applied. Then, to produce a bubble at the aperture of the cantilever, a positive pressure of 200 mbar was applied inside the microfluidic cantilever immersed in the buffer. The silanized probes were calibrated using the thermal noise method before each measurement [51]. The interactions between the bubbles produced and PES-PBS or PES-VAN membranes were then recorded in force spectroscopy mode using a maximum applied force of 1.2 nN, a constant approach retraction speed of 3.0 µm/s, and a delay time of 1.0 s. For each membrane, several areas of 4 x 4 µm were probed. Adhesion forces were obtained by calculating the maximum adhesion force on the retract force curves.

3. Results and discussion

3.1. Membrane coating with vanillin

In the first step of the study, we optimized the conditions to provide membranes coated with vanillin. PES membranes are negatively charged and hydrophilized to ensure low protein binding capacities (specifications from the provider, https://www.3m.com). Their high permeability comes from a highly asymmetric porous structure. Vanillin is a slightly hydrophobic molecule (log Kow = 1.23, OECD data) depending on the pH of the solution. At pH 3.8, vanillin is mainly in its protonated form ensuring maximum coating densities by reducing electrostatic repulsion with the sulfur oxygen groups of the PES membrane. Moreover, in this condition, hydrophobic interactions are enhanced between the different vanillin groups and PES phenyl rings and the OH groups of the vanillin can H-bond with the sulfur oxygens of the PES [46]. For these reasons, pH 3.8 was chosen for the membrane coating step.

The first objective was to define the transmembrane pressure (TMP) that would result in a homogeneous and high vanillin quantity on the membrane surface while minimizing the decline in transfer properties of the membrane. The effect of varying TMP (0.05 bar, 0.1 bar, 0.2 bar, and 0.4 bar) on coating quantity and membrane performance (pure water flux decline) before and after the membrane modification was investigated. A previous study by Virtanen *et al.* (2018) demonstrated that PES-vanillin interaction (graphical abstract) occurs in two timescales [46] (Figure S1). At a rapid timescale, the dominant interaction is the hydrophobic ones between the aromatic rings of vanillin and of PES. At a slower timescale, the OH group of vanillin H-bonds with the sulfur oxygens of PES and vanillin disperses from each other which leads to an even coating coverage on the PES surface. In this study, the effect of pressure resulted in two general trends in the obtained coating quantity and pure water flux (Figure 2A). Pure water permeability results are presented in Figure S2. At higher TMP, 0.2 and 0.4 bar, the coating quantities were lower and comparable with each other (249 ± 5 and 237 ± 25 $\mu g.cm^{-2}$, respectively), while the pure water flux decline ratios (FDR) were close to unity (1.09 and 1.01, respectively) indicating that the membrane performance is retained even after surface modification. At these pressures, the hydraulic conditions are stronger. Consequently, as per the previous study by Virtanen *et al.*, it could mean that there is insufficient time to form stronger PES-vanillin interaction (H-bond) and the hydrophobic interactions between the aromatic rings of PES and vanillin are more dominant. Vanillin, therefore, gets flushed through the membrane's porous structure which explains the retention of membrane performance as demonstrated by FDR values close to 1. While at lower TMP, 0.05 and 0.1 bar, the coating quantity significantly increased to 546 ± 34 and 337 ± 15 $\mu g.cm^{-2}$, respectively. When working at lower TMP, vanillin accumulation in the porous structure is facilitated by lower hydraulics thereby increasing the probability of adsorption of vanillin molecules on the membrane surface. This could also imply that there is sufficient time for the vanillin to form both hydrophobic and H-bond interactions with the PES and distribute evenly to the PES surface. This was evident in the decrease of pure water flux after modification (lower FDR values). Although 0.05 bar TMP demonstrated the highest coating quantity, the membrane performance was significantly reduced with the lowest FDR of 0.63 ± 0.07 compared to 0.1 bar with an FDR of 0.86 ± 0.14. For this reason, 0.1 bar TMP was chosen as a good compromise as it has a relatively high coating quantity with a minor membrane performance loss of only 14%. From this result, we assume that the coating will not have a significant impact on the pore size.

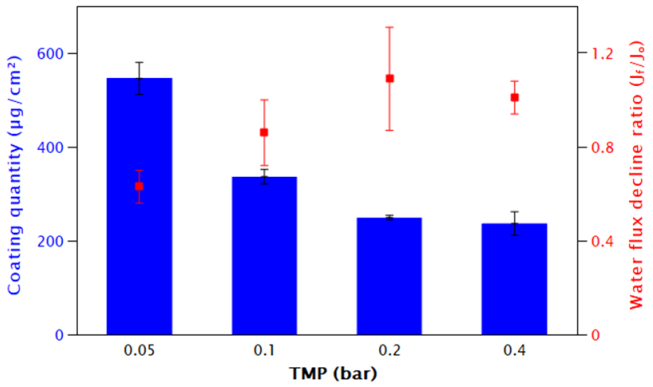

Figure 2. *Coating quantity (histogram) and pure water flux decline ratio (FDR, dots) of PES-VAN membranes filtered with 2000 mL of 3g.L^{-1} vanillin solution at varied transmembrane pressure (TMP)*

The FTIR maps generated at 1511 cm^{-1}, which corresponds to the aromatic ring of vanillin, and IR peaks absorbance ratio confirmed the presence and coverage of vanillin on the PES surface at varied TMP (Figure 3A-F). The full IR spectra of the samples, highlighting the relevant peaks for their respective chemical groups are presented in supplementary data (Figure S1). Pristine PES membrane has blue color only, implying that there is no vanillin present on their surface. These results agree with the obtained coating quantity. In addition, the relationship between the average peak height intensity of the FTIR maps and the coating quantity is non-linear as shown in Figure 3G. A linear correlation, represented by the dashed line, was chosen assuming that at high pressure, vanillin was retained and adsorbed only at the surface. The points falling below the dashed line show that at lower pressure, 0.1 and 0.05 bar, we observe a deviation in the total quantity adsorbed compared to the coating coverage on the surface as observed through the FTIR mapping. This deviation indicates that a portion of vanillin penetrates through the membrane and adsorbs into the pores at low pressure. This agrees with the literature where Virtanen *et al.* [46] showed that vanillin penetrated a few nanometers deep into the PES membrane when it was modified via cross-flow filtration. Moreover, the depth of penetration of FTIR-ATR analysis is usually in a few micrometer range, approximately 3-5 µm using diamond crystal [9]. This implies that at lower TMP, the vanillin has more time to adsorb into the depth of the membrane for more than a few micrometers. This could also explain the flux decline under these conditions. Nevertheless, despite vanillin penetration through the membrane, FTIR maps show that at 0.1 bar, a homogeneous coating coverage on the membrane surface was still achieved. In conclusion, after consideration of vanillin coating quantity, coating coverage on the membrane surface, and membrane performance, a TMP of 0.1 bar will be used for the following experiments.

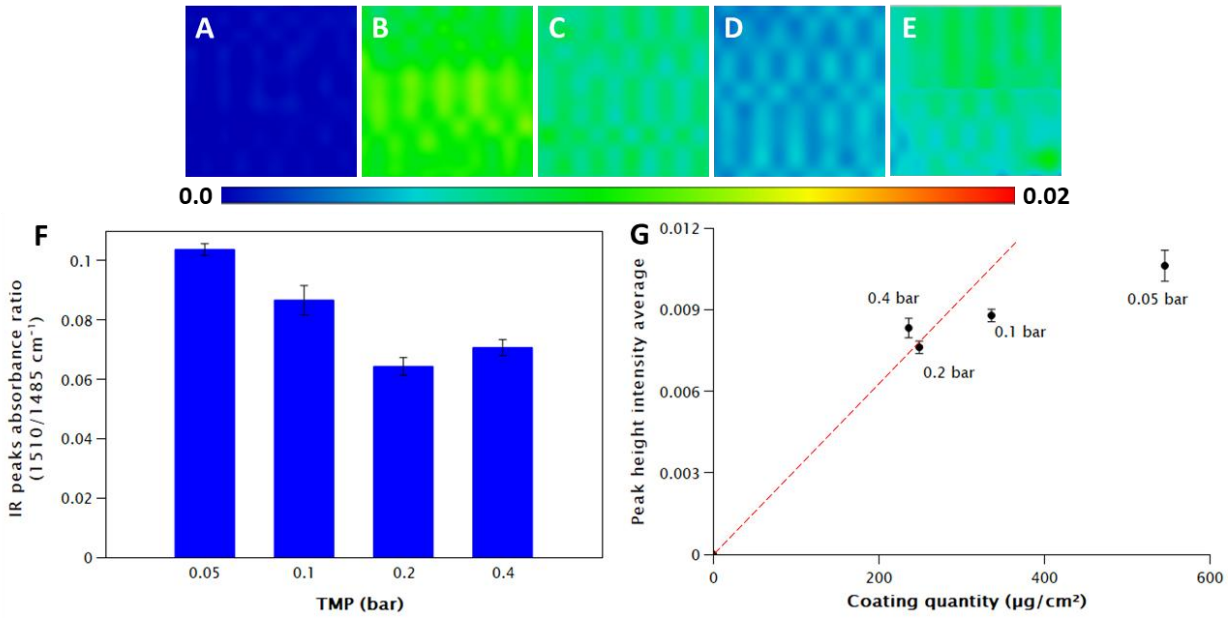

Figure 3. *FTIR maps generated at 1511 cm^{-1} of A) pristine PES membrane, PES-VAN at B) 0.05 bar, C) 0.1 bar, D) 0.2 bar, and E) 0.4 bar TMP. Each map has an area of 0.25 mm^2. The vanillin concentration used was 3g.L^{-1} and filtrate volume of 2000 mL. F) Mean absorbance ratio of the vanillin to the PES membrane peaks (1510 and 1485 cm^{-1}, respectively) as a function of the TMP applied during the filtration of 2000 mL of 3 g.L^{-1} vanillin solution. G) Peak height intensity average from FTIR maps as a function of the coating quantity; the dashed line represents the hypothetical correlation for which vanillin is adsorbed only at the membrane surface.*

The stability of PES membranes modified with vanillin at 0.1 bar was also evaluated. Results showed that 41% (138 ± 29 µg.cm^{-2}) and 34% (115 ± 26 µg.cm^{-2}) of vanillin was retained after stirring and filtration desorption tests, respectively (Figure 4). Although a portion of vanillin was removed, the quantity left was sufficient to minimize biofouling in single-cell scale and population scale adhesion studies (sections 3.3 and 3.4).

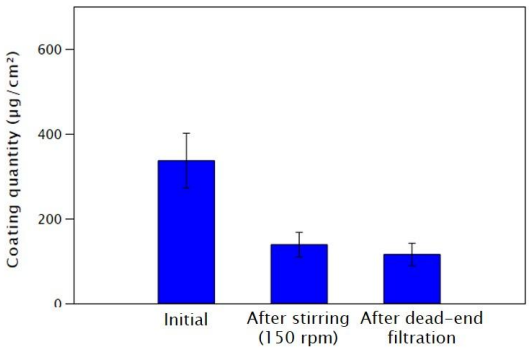

Figure 4. *Vanillin coating quantity on PES-VAN membranes before and after desorption assays under stirring or dead-end filtration mode (three hours and 2000 mL of ultrapure water).*

3.2. Characterization of the surface modification

According to the literature, surface modification with vanillin renders the surface hydrophilic with static contact angles ranging from 30 to 55° [42-44]. These results are not coherent with the inherent

hydrophobic nature of vanillin and no significant gain in the pure water permeability was observed. Shin *et al*. (2020) reported a 10% decrease in pure water permeability after the modification [43] and Katebian *et al*. (2018) showed that there is no statistical difference in the water permeability before and after the modification [44]. The change in the measured contact angles of the membrane surface can depend on several factors: the new properties that the vanillin imparts and the rugosities created by the deposition or accumulation of the molecule on the surface. Consequently, the combination of these may not be measurable through macroscopic characterization such as water flux making it challenging to isolate the nature and mechanisms of the membrane performance. In addition, parameters from filtration tests may also be dependent on complex membrane internal structure. For these reasons, this section will be devoted to the local characterization (in nano- and micrometer scale) of membrane properties after coating at 0.1 bar.

Both roughness and hydrophilicity have to be considered to assess the effect of surface modification on bacterial adhesion. Atomic force microscopy was further used to characterize the PES-PBS and PES-VAN membranes. AFM height images of the membrane surfaces are presented in Figure 5A and C. The estimated apparent pore sizes measured from these images did not decrease after surface modification (Figure S3), which was also verified on SEM images (Figure S4). This further confirms our previous assumption at section 3.1 that the vanillin coating will not have a significant impact on the pore size. Furthermore, although the pores of the membranes are clearly visible in the images, it is difficult to conclude from these images whether vanillin (effective diameter in water is 6 Å [57]) is present or not on the membrane surfaces. We thus performed roughness measurements on these membrane surfaces, on areas of 500 x 500 nm located between the pores. Examples of the images used for roughness measurements are presented as supplementary information (Figure S5). Filtration of vanillin increased the surface roughness (Figure 5B, full data are in Supplementary table 1). From 1.5 ± 0.2 nm, indeed, at 71 ± 12 $\mu g.cm^{-2}$ of vanillin, the roughness slightly increased to 1.6 ± 0.2 nm and at 105 ± 28 $\mu g.cm^{-2}$ of vanillin, the increase in roughness became significant (Mann and Whitney test, $p \leq 0.05$), to 1.9 ± 0.2 nm. This increase in roughness is attributed to the deposition of vanillin on the membrane surface especially at larger volumes of vanillin solution. Indeed, the presence of vanillin on the membrane surface was verified by other characterization techniques such as FTIR mapping and FTIR-ATR (section 3.1).

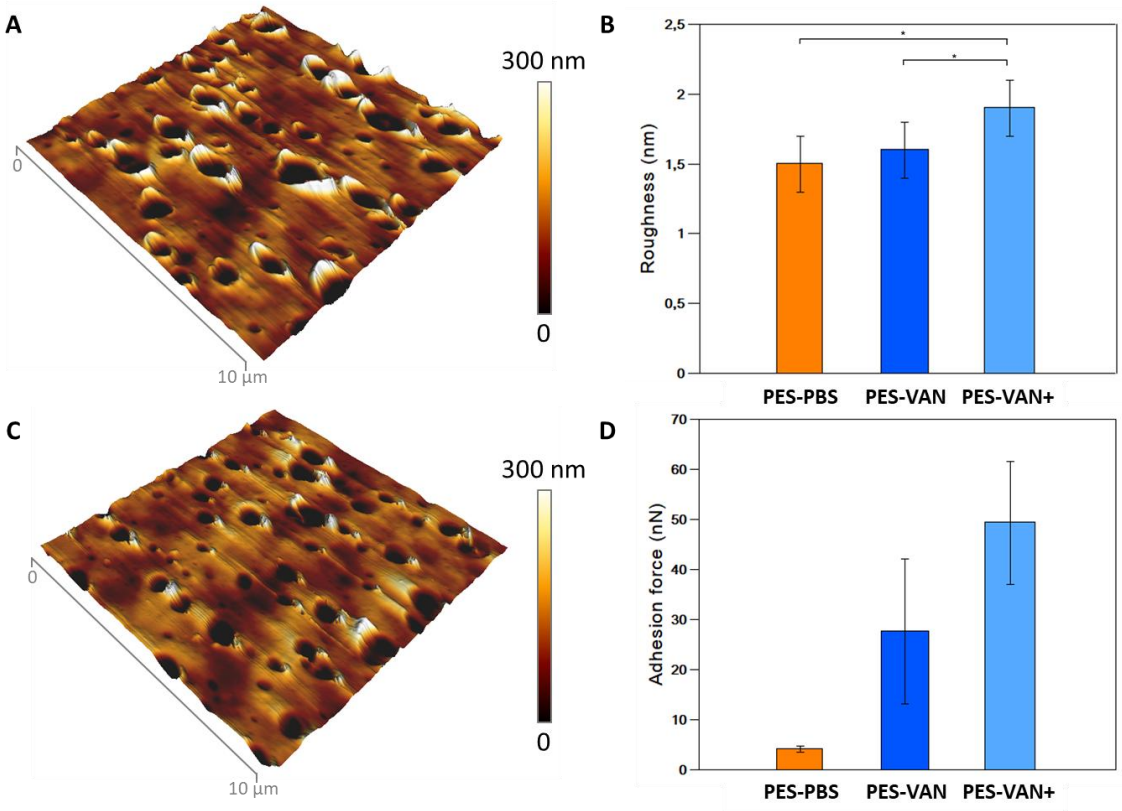

Figure 5. *AFM 3D height images of areas of 10 x 10 µm² on the surface of (A) PES-PBS membrane and (C) PES-VAN+ membrane containing 105 ± 28 µg.cm^{-2} of vanillin. Roughness measurements were performed on 500 x 500 nm² areas between the pores of the membranes; the histogram in (B) shows the quantification of these measurements. Lastly, the interactions between membranes and a bubble probe were performed using FluidFM; the histogram in (D) shows the average adhesion forces recorded in each case.*

In addition, AFM was used to characterize the hydrophobicity of the membranes used in this study. For that, their interactions with a bubble probe produced using FluidFM technology [56] were measured. As bubbles behave like hydrophobic surfaces, the forces recorded then directly reflect the hydrophobicity of the materials probed. The results showed that the adhesion force recorded increased with the amount of vanillin filtered on the membranes (Figure 5D). From approximately 5 nN for untreated or PES-PBS membranes, the adhesion force increased to 27.6 ± 14.5 nN for PES-VAN membrane with a coating quantity of 71 ± 12 µg.cm^{-2}, and to 49.3 ± 12.3 nN for PES-VAN+ membrane with coating quantity of 105 ± 28 µg.cm^{-2}. This increase in the adhesion force indicates that vanillin modifies the physical-chemical properties of the membranes and renders them hydrophobic, with more vanillin adsorbed on the membranes resulting in a higher hydrophobicity of the material. These results are in accordance with water contact angle measurements performed on these membranes. WCA was found to increase with vanillin coating quantity, from 65.2 ± 4.4° for the PES-PBS membrane to 75.7 ± 2.8° for the PES-VAN membrane (coating quantity of 142 ± 25 µg.cm^{-2}). The increase in hydrophobicity could also explain the slight decrease in pure water flux upon increase of vanillin quantity on the membrane surface. Our results combining the water contact angle and AFM measurements provide an answer to the contradictory results found in literature. Indeed, Esmaeili *et al.* [42] showed that contact angle increased at higher vanillin concentration while Kumar *et al.* [45] and Shin *et al.* [43] demonstrated the opposite. Considering that

contact angle measurements are influenced not only by the material surface's intrinsic physical-chemical properties but also by the surface topography, it is challenging to use this method in identifying the surface's inherent property, thus, resulting in varying degrees of hydrophilicity. Using AFM for hydrophobicity measurement offers an advantage to study the surface locally in the micrometer range in comparison with contact angle measurements with bubble sizes in the millimeter range. This method revealed the inherent hydrophobic nature of vanillin as a result of the surface modification strategy used on the membrane and highlighted the fact that despite a subnanometer scale change in surface roughness, it had a significant effect on hydrophobicity. In addition, a small-scale study like this could be more advantageous in understanding bacterial interaction as they happen on a smaller scale.

3.3. Initial adhesion of bacteria measured at the cell scale by AFM

To answer the question of whether or not vanillin could have a potential effect on the initial attachment of bacterial cells onto the surfaces, we decided to directly probe, using AFM, the interactions between single cells and the different membranes produced in this study. *P. aeruginosa* was chosen as it rapidly produces biofilm to attach over surfaces, and biofilm maturation was found to be interconnected with quorum sensing activities [58]. Hence, it is expected to be sensitive to vanillin as a quorum sensing inhibitor and represents a bacteria strain model for biofilm development control. In these experiments, we used the single-cell force spectroscopy technique, which consists in attaching one bacterial cell to a colloid AFM cantilever, making it then possible to probe the interactions between this bacterial cell and a surface in force spectroscopy mode. This gives access to force *vs* distance curves, from which information can be extracted. The adhesion force, which quantifies the force needed to break the interaction between the cell and the surface, is a direct reflection of the possibility of the cell to adhere to the material or not. It can be calculated from the force curves by measuring the height of the biggest retract adhesion peak visible on the force curves. Such calculations are then realized for arrays of force curves (400 in our case) recorded at the surface of membranes (Figure 6). In the case of PES-PBS membranes (Figure 6A), the force curves recorded show multiple retract adhesions, meaning most likely that polymers from the bacterial cell surface are unfolded upon retraction of the AFM cantilever. Indeed, physical-chemical forces such as electrostatic or hydrophobic are usually materialized by a single peak taking place at the contact point [59], whereas multiple peaks distributed over the retract curve on long distances are usually due to the successive unfolding of polymer sub-units such as polysaccharide present at cell surfaces [60]. The adhesion force recorded in this case was 275.5 ± 160.6 pN, and only 6.1 % of the force curves recorded did not present adhesive events. On PES-VAN membranes with a vanillin coating quantity of 71 ± 12 $\mu g.cm^{-2}$, the adhesion force recorded was similar (263.9 ± 141.4 pN); however, the force curves recorded did not present multiple interactions unlike for PES-PBS membranes, meaning that probably fewer molecules from the cell surface are involved in the interactions. Another important difference is in the adhesion percentage, as the % of non-adhesive curves recorded increased to 11.3%. Such increase is even more important for PES-VAN+ membranes with a vanillin coating quantity of 105 ± 28 $\mu g.cm^{-2}$, as 38.4% of the force curves did not present adhesive events anymore. In addition, in this case, the adhesion force significantly decreased to 178.2 ± 98.7 pN (independent student test, $p \leq 0.001$). Adhesion forces obtained and % of adhesion are summarized in Figure 6D and E, respectively. From these results, it is then clear that the presence of vanillin on the surface of the membranes affects both the probability of cells to adhere to the surface and the adhesion forces. This has important implications, as this decrease in the adhesion force means that a small flux might be able to detach cells from the surface, thus alleviating the cleaning procedures.

Biofilm formation on surfaces usually involves three steps. The first step consists of the reversible adhesion of cells to surfaces, followed by irreversible microbial adhesion [61] where physical-chemical bonds between cells and the surface are strengthened. Finally, after these adhesion steps, cells undergo important changes (cell wall deformation, production of exopolysaccharides, gene expression, etc.) which

lead to the formation of a mature biofilm [62]. In this work, only the first step was assessed, the initial adhesion to the surface. This step can be influenced by different surface properties, such as surface charge, roughness, or hydrophobicity [63]. AFM measurements were performed on PES-PBS and PES-VAN membranes submerged in PBS at a pH 7.4. In these conditions, vanillin (pKa = 7.4) exists in both protonated and unprotonated forms and the PES membrane (pHi = 7) exhibits negative charges which is favorable to the electrostatic repulsion of bacteria that are negatively charged [64]. An increase in adhesion of microorganisms is generally observed when the surface roughness increases to the micrometer scale [3, 65]. In our case, the roughness changes induced by the incorporation of vanillin are in the subnanometer scale. Nevertheless, a decrease in the adhesion of *E. coli* cells in static condition was observed on surfaces with increased roughness at the subnanometer scale [66] which is more similar to our experimental conditions. In addition, previous studies have shown that when the sizes of surface patterns are smaller than the bacterium such as *P. aeruginosa*, the adhesion is significantly reduced [3]. A theoretical model, based on extended Derjaguin-Landau-Verwey-Overbeek (XDLVO) theory, showed that the contribution of electrostatic interactions to the total interfacial interaction was found to be minimal on smooth surfaces. However, when surface roughness in nanometer range was considered, the contribution of electrostatic repulsion increased [67] and could end up in an easier detachment of the bacteria from the surface [68]. This is in line with the results obtained during AFM force spectroscopy measurements, which showed a reduced adhesion force on vanillin-coated membranes, which could result in easier bacterial detachment. Regarding hydrophobicity, some studies have shown a stronger attachment of bacteria to hydrophobic surfaces [64, 69, 70]. Vanillin-modified membranes are more hydrophobic compared to the control membranes, and yet, the cell adhesion was reduced. First, this means that the anti-adhesion effect is stronger than a potential attractive effect caused by an increased hydrophobicity, and second that the anti-adhesion effect could be also due to the biochemical effect of vanillin which affects bacterial cell surface integrity via pH homeostasis loss as observed in *L. plantarum, L. innocua,* and *E. coli* [36] or even in *M. smegmatis* [35] which has a more complex cell wall core. A previous study also demonstrated that damage to the cell surface of *P. aeruginosa* could decrease its capacity to adhere to a hydrophobic surface [71, 72]. When disrupted, the bacteria cell wall itself undergoes a change in its surface properties, releasing lipid components from the cell, and cell wall stress also induces the inhibition of EPS production via cyclic adenosine monophosphate (cAMP) signaling during cell wall repair [73].

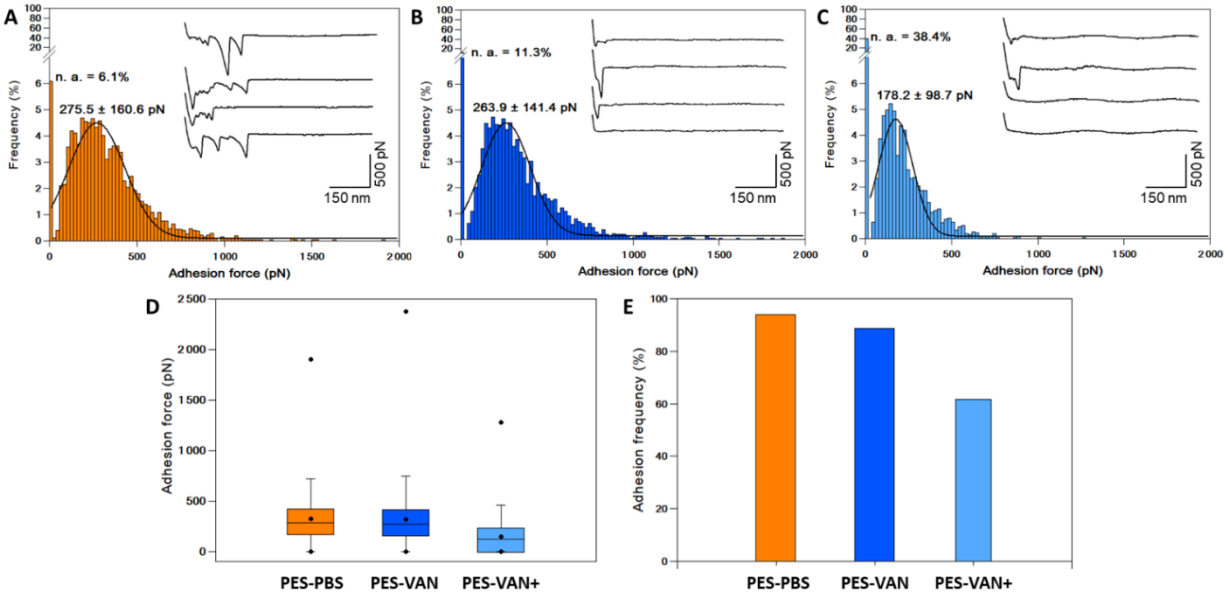

Figure 6. *Interactions of P. aeruginosa cells with membrane surfaces. Histograms showing the distribution of adhesion forces recorded between single P. aeruginosa cells and (A) PES-PBS membranes, (B) PES-VAN membrane containing 71 ± 12 µg.cm^{-2} of vanillin, and (C) PES-VAN+ membrane containing 105 ± 28 µg.cm^{-2} of vanillin. In each case, insets show representative force curves. The results presented come, in each case, from 7 cells from 3 independent cultures. (D) Box-plot summarizing the adhesion force results and (E) histogram summarizing the percentages of adhesion recorded in each case.*

3.4. Adhesion of bacteria at the population scale

In the frame of our study, the bacterial adhesion at the initial stage of biofilm development is required to understand the impact of the physical-chemical surface modifications. Thus, we investigated the effects of vanillin at the cell population scale using adhesion assays of *Pa* in contact with the membranes for 3h. This was performed with the objective to distinguish the effect of vanillin on the initial adhesion of bacteria from the biofilm development wherein EPS are present. For this purpose, we developed a different protocol than the one usually performed in the literature [74] which does not differentiate bacterial adhesion from sedimentation. For that, we used inserts placed upside down in the suspension, as described in the material and methods, section 2.4. The adhesion of bacteria was also evaluated under agitation and static conditions on virgin PES membrane placed in a multi-well culture plate as classically performed. Moreover, instead of detaching the adhered bacteria from the membrane surface by ultrasonic treatment for enumeration, in our case, we quantified the adhered bacteria directly on membrane surfaces using epifluorescence microscopy. This way we could determine the bacterial coverage rate using image analysis [75].

First, we validated this new protocol by comparing the bacterial coverage rate (i) obtained under static conditions (0 rpm) with the one obtained under agitation (150 rpm), and (ii) depending on the position of the PES-PBS membrane in the culture plate well, allowing the sedimentation of bacteria (at the bottom) or not (in the insert). Looking at the effect of agitation on PES-PBS membranes placed at the bottom of the well (Figure 7E and F), under agitation of 150 rpm, the bacterial coverage rate for the membranes was on average 0.61 ± 0.41%, while in the absence of agitation, the mean coverage rate was 1.03 ± 1.29%. The absence of agitation led to a 69% increase in the mean coverage rate and high heterogeneity in the values obtained for the membranes placed at the bottom of wells (Figure 7A, C, and F). Agitation had no significant effect on the coverage rate of the membranes placed in the inserts; in fact, the mean coverage rate was 0.29 ± 0.29% with 150 rpm of agitation and 0.27 ± 0.24 % without agitation, highlighting the importance of our approach to differentiate between bacterial adhesion and sedimentation. These results imply that hydrodynamic conditions induced by plate agitation affect the bacterial colonization of the PES membrane surface less when placed in the inserts. In addition, diffuse fluorescence around the cells was observed in conditions under agitation, which suggests the presence of extracellular DNA. Therefore, biofilm formed more rapidly in response to hydrodynamic stress [52, 76]. The use of inserts without agitation allows clear visualization of the cells on the surface of the samples and a better estimation of the initial adhesion before the production of EPS in the tested experimental conditions (Figure 7D). Thus, adhesion assays were performed for 3h in PBS 1X (pH 7.4) as a holding medium, with the use of inserts and without agitation. In this condition, the probability of adhesion is reduced to natural convection, diffusion, and motility of the bacteria to the membrane surface. This means that after potential repulsion of the bacteria from the membrane surface due to a change in surface properties, only irreversibly adhered bacteria will stay attached after rinsing. In addition, these conditions do not promote biofilm formation due to the absence of stress conditions.

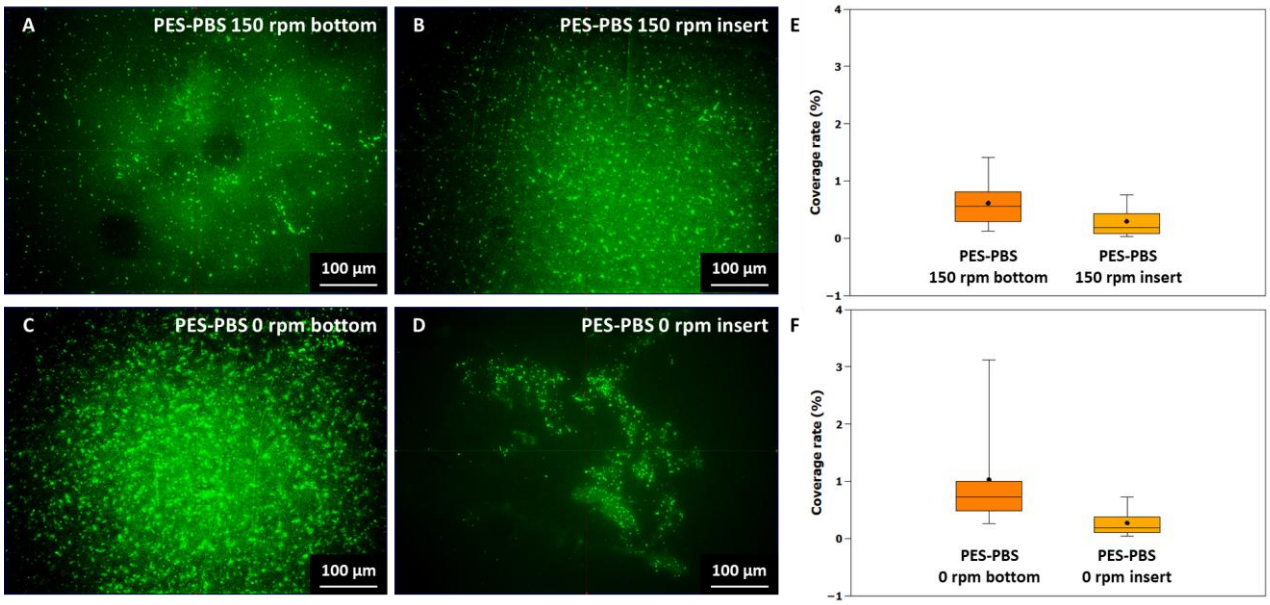

Figure 7. *Effect of agitation and sedimentation on the bacterial colonization of PES membranes. Epifluorescence microscopy (EFM) images of bacterial adhesion assays on PES-PBS membrane surface under different conditions stained with SYBR™ Green: (A) agitation at 150 rpm with the membrane at the bottom of the well, (B) agitation at 150 rpm with the use of insert, (C) static condition with the membrane at the bottom of the well, and (D) static condition with insert. (E, F) Box and whisker plots showing the coverage rates by P. aeruginosa on PES membranes and quantification in EFM with ZEN blue image analysis tools.*

After these adhesion tests, the membrane coupons were prepared for scanning electron microscopy to observe the morphology of the bacteria present on the membranes. SEM observations showed similar morphologies between bacteria adhered to PES-PBS and PES-VAN membranes (Figure 8). However, a lower density of bacteria on the surface of PES-VAN membranes was observed (Figure 8B and D). The presence of filaments in the vicinity of *P. aeruginosa* cells was clearly observed on the PES-PBS membranes (Figure 8A and C) whereas these same filaments were almost invisible on the vanillin-modified membranes (Figure 8B and D), probably due to their thinness. These filaments could correspond to EPS filaments and the presence of vanillin seems to affect their quantity and/or structure.

Observations were also carried out in epifluorescence microscopy with the highest coating quantity obtained in this study, 193 µg.cm^{-2} (Figure 9). They showed that, from a qualitative point of view, the microbial density at the surface of the PES-VAN membranes is significantly lower than on the PES-PBS membranes, which is consistent with the observations made in SEM. It was further confirmed by the quantification of the bacterial coverage rate carried out by analyzing a total of 78 images. The coverage rate of *P. aeruginosa* on PES-PBS membrane was 0.82 ± 0.74%, while 0.42 ± 0.39% for the PES-VAN membrane. The bacterial coverage rate on PES-VAN membranes was reduced by 50% compared to the PES-PBS membranes (p-value < 0.05, Welch test, Figure 9C). Therefore, the presence of vanillin adsorbed on the membrane surface with a coating quantity of 193 µg.cm^{-2} affects the initial adhesion by decreasing the coverage rate of adhered bacteria to the surface by half after 3h adhesion assay. Moreover, it seems that the quantity, quality, and/or structure of the EPS were also affected by the presence of vanillin, confirming the results from SEM. At pH 7.4, the vanillin is half protonated and could desorb slowly from the surface. In the worst case, if all the vanillin desorbs, the estimated concentration of vanillin in the solution would be less than the value required to produce a deleterious or QSI effect on

bacteria [32, 33, 36]. The results obtained then demonstrated that in our experiments the QSI effect can be mainly attributed to the vanillin remaining adsorbed on the membrane surface.

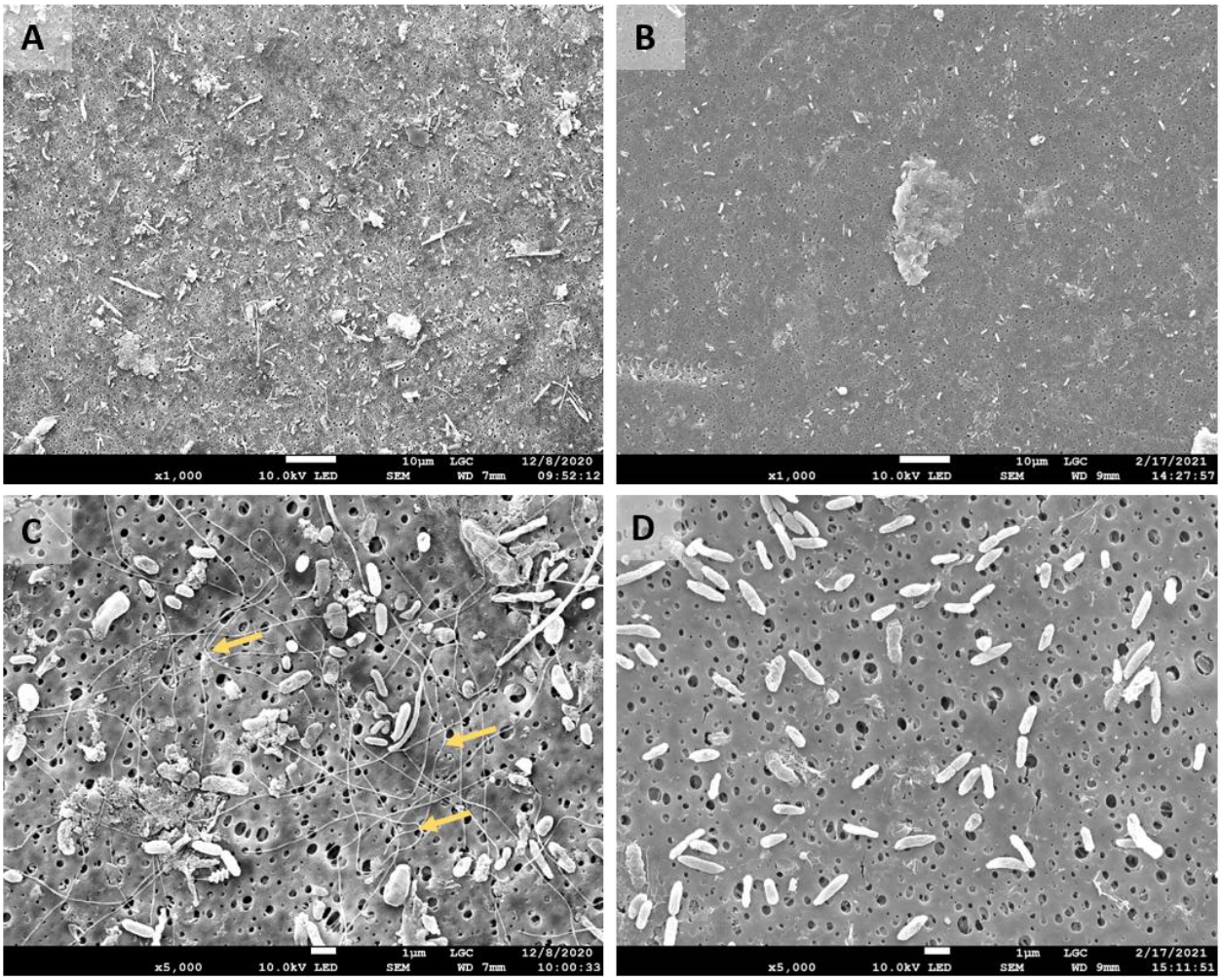

Figure 8. *SEM images of (A x1000, C x5000) PES-PBS and (B x1000, D x5000) PES-VAN membranes (vanillin coating quantity of 142 ± 25 µg.cm^{-2}) after 3h adhesion assay.*

The 3h adhesion assay corresponds to the bacterial irreversible adhesion stage of biofilm formation at the membrane surface. These results showed that even with such short contact time (3h) of *P. aeruginosa* with the membrane in control conditions (PES-PBS membrane), EPS were produced and bacteria adhered to the membrane surface. This results from a cascade of signaling molecules (proteins) expressed shortly after the incubation (occurs in less than 2 hours) which are responsible for the rapid attachment kinetics of the bacteria after its first contact with the surface [73, 77]. For QS mechanisms to take place, it is required that numerous bacteria attach to the surface to induce EPS production and initiate biofilm formation [78-80]. In the case of PES-VAN membranes, not only the adhesion of bacteria is reduced but also the production of EPS is affected by the presence of vanillin at the membrane surface. Previous studies have shown that vanillin leads to a modification of EPS components with a decrease in exopolysaccharides and exoproteins [37, 41], via QSI [32, 33], which is in agreement with the present results. Also, it is not surprising that no induction of the QS mechanisms responsible for EPS production and biofilm development was observed when the number of bacteria adhered to the membrane surface decreased. It thus confirms that the homeostatic and quorum sensing inhibitory effect of vanillin for the gram-negative bacteria are effective already at the first stage of bacterial adhesion and biofilm development.

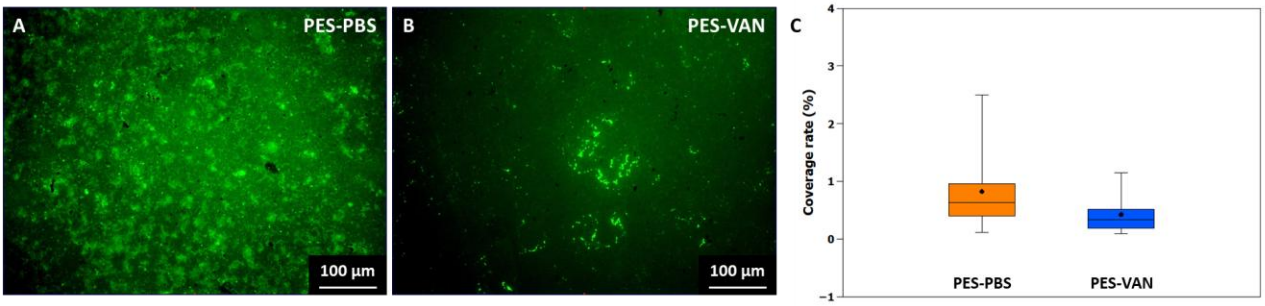

Figure 9. *Epifluorescence microscopy images of PES membrane surface labeled with SYBR™ Green: (A) PES-PBS and (B) PES-VAN (vanillin coating quantity of 193 µg.cm^{-2}) membranes after 3h adhesion assay, and (C) corresponding box and whisker plot showing the coverage rates of P. aeruginosa on PES-PBS and PES-VAN membranes and quantification in EFM with ZEN blue image analysis tools.*

4. Conclusion

Modified PES membranes were obtained by dead-end filtration of vanillin solution. The vanillin-coated membranes, PES-VAN, were characterized in terms of filtration performances, physical-chemical surface properties, and adhesion of bacteria at the cell and population scales. For this, a new method for bacterial adhesion assay was developed and a combination of characterization techniques at different size scales, from macro- to nanoscale, was performed to validate the multifunctional effects of vanillin.

The results from this study conclude that:

- The coating of vanillin by filtration was optimized by decreasing the flux through the membrane at low transmembrane pressure.
- Small-scale localized measurements using AFM revealed the inherent hydrophobicity of PES-VAN membranes and that there is only subnanometer scale change in surface roughness. This was correlated to the membrane's macroscale property wherein a small reduction in membrane permeability was observed.
- The new method for bacterial adhesion assay by using inserts to support membranes avoids the sedimentation effect on bacterial attachment and promotes only the initial stage of biofilm development. Moreover, it reduces DNA fragment deposition and optimizes the observation and quantification of bacterial adhesion on the membrane surface.
- The combination of multiscale (from micro- to nanometer scale) characterization strategies using AFM, EFM, and SEM demonstrated that vanillin on the membrane's surface: (i) reduces the adhesion forces and the probability of the cells to adhere to the surface at the initial stage of biofilm development, and (ii) affects the structure and development of the biofilm.

Altogether, the combination of multiscale characterization methods demonstrated how vanillin minimizes biofouling on membranes, which intervenes at different levels of biofilm development from surface colonization and adhesion of bacteria to the early stages of biofilm formation. These results show that vanillin adsorption on the membrane surface will limit the bio-adhesion and biofouling during filtration processes and will facilitate and alleviate the cleaning procedures usually required. In addition, the proposed surface modification method in this study offers advantages. The use of dead-end filtration is fairly simple and adaptive to water treatment applications. Consequently, it can be easily scaled up and vanillin could be reloaded as needed making it suitable for an industrial setting.

Supplementary Information (SI)

The supplementary information provides examples of the images and cross-section profiles used for roughness measurements in AFM.

Declaration of competing interest

The authors declare that they have no known competing financial interests or personal relationships that could have appeared to influence the work reported in this paper.

Author statement

Nadège Durban-Benizio, Abigail Burato Rosales, Xuan Loc Nguyen, Clémentine Lamo: Methodology, Formal analysis, Investigation, Writing

Irem Demir-Yilmaz: Methodology, Formal analysis, Investigation

Vincent Bouvier: technical support, data acquisition

Christel Causserand: Writing, review

Cécile Formosa Dague: Conceptualization, Supervision, Funding acquisition, Writing - review & editing

Clémence Coetsier: Conceptualization, Supervision, Funding acquisition, Writing - review & editing

Acknowledgements

This work was supported thanks to funds from Agence nationale de la Recherche (ANR), JCJC project BIOCOM ANR-17-CE04-0001 to C. Coetsier, and JCJC project FLOTALG ANR-18-CE43-000101 to C. Formosa-Dague. The authors would like to thank Marie-Line de Solan-Bethmale and Sandrine Desclaux from LGC for the SEM images acquisition, the ICT platform and especially Corine Routaboul for FTIR measurements.

References

[1] Y. Luo, W. Guo, H.H. Ngo, L.D. Nghiem, F.I. Hai, J. Zhang, S. Liang, X.C. Wang, A review on the occurrence of micropollutants in the aquatic environment and their fate and removal during wastewater treatment, Science of The Total Environment, 473–474 (2014) 619-641.

[2] J.L. Acero, F.J. Benitez, F. Teva, A.I. Leal, Retention of emerging micropollutants from UP water and a municipal secondary effluent by ultrafiltration and nanofiltration, Chemical Engineering Journal, 163 (2010) 264-272.

[3] C. Berne, C.K. Ellison, A. Ducret, Y.V. Brun, Bacterial adhesion at the single-cell level, Nature Reviews Microbiology, 16 (2018) 616-627.

[4] Y. Ren, C. Wang, Z. Chen, E. Allan, H.J. Busscher, H.C. van der Mei, Emergent heterogeneous microenvironments in biofilms: substratum surface heterogeneity and bacterial adhesion force-sensing, FEMS Microbiology Reviews, 42 (2018) 259-272.

[5] M. Aslam, R. Ahmad, J. Kim, Recent developments in biofouling control in membrane bioreactors for domestic wastewater treatment, Separation and Purification Technology, 206 (2018) 297-315.

[6] H.C. Flemming, G. Schaule, T. Griebe, J. Schmitt, A. Tamachkiarowa, Biofouling—the Achilles heel of membrane processes, Desalination, 113 (1997) 215-225.

[7] A. Ghosh, R. Bindal, S. Prabhakar, P. Tewari, Composite Polyamide Reverse Osmosis (RO) Membranes–Recent Developments and Future Directions, BARC Newsletter, 321 (2011) 43-51.

[8] B. Pellegrin, E. Gaudichet-Maurin, C. Causserand, Mechano-chemical ageing of PES/PVP ultrafiltration membranes used in drinking water production, Water Science & Technology: Water Supply, 13 (2013) 541-551.

[9] B. Pellegrin, R. Prulho, A. Rivaton, S. Thérias, J.-L. Gardette, E. Gaudichet-Maurin, C. Causserand, Multi-scale analysis of hypochlorite induced PES/PVP ultrafiltration membranes degradation, Journal of Membrane Science, 447 (2013) 287-296.

[10] H. Xu, K. Xiao, X. Wang, S. Liang, C. Wei, X. Wen, X. Huang, Outlining the Roles of Membrane-Foulant and Foulant-Foulant Interactions in Organic Fouling During Microfiltration and Ultrafiltration: A Mini-Review, Frontiers in Chemistry, 8 (2020).

[11] Y.-X. Shen, P.O. Saboe, I.T. Sines, M. Erbakan, M. Kumar, Biomimetic membranes: A review, Journal of Membrane Science, 454 (2014) 359-381.

[12] D. Rana, T. Matsuura, Surface Modifications for Antifouling Membranes, Chemical Reviews, 110 (2010) 2448-2471.

[13] V. Kochkodan, N. Hilal, A comprehensive review on surface modified polymer membranes for biofouling mitigation, Desalination, 356 (2015) 187-207.

[14] N.P. Gule, N.M. Begum, B. Klumperman, Advances in biofouling mitigation: A review, Critical Reviews in Environmental Science and Technology, 46 (2016) 535-555.

[15] R. Sengur-Tasdemir, S. Aydin, T. Turken, E.A. Genceli, I. Koyuncu, Biomimetic Approaches for Membrane Technologies, Separation & Purification Reviews, 45 (2016) 122-140.

[16] Y. Xiong, Y. Liu, Biological control of microbial attachment: a promising alternative for mitigating membrane biofouling, Applied Microbiology and Biotechnology, 86 (2010) 825-837.

[17] G. Li, G. Cheng, H. Xue, S. Chen, F. Zhang, S. Jiang, Ultra low fouling zwitterionic polymers with a biomimetic adhesive group, Biomaterials, 29 (2008) 4592-4597.

[18] F. Ghilini, D.E. Pissinis, A. Miñán, P.L. Schilardi, C. Diaz, How Functionalized Surfaces Can Inhibit Bacterial Adhesion and Viability, ACS Biomaterials Science & Engineering, 5 (2019) 4920-4936.

[19] R. Malaisamy, D. Berry, D. Holder, L. Raskin, L. Lepak, K.L. Jones, Development of reactive thin film polymer brush membranes to prevent biofouling, Journal of Membrane Science, 350 (2010) 361-370.

[20] W. Choi, C. Lee, D. Lee, Y.J. Won, G.W. Lee, M.G. Shin, B. Chun, T.-S. Kim, H.-D. Park, H.W. Jung, J.S. Lee, J.-H. Lee, Sharkskin-mimetic desalination membranes with ultralow biofouling, J. Mater. Chem. A, 6 (2018) 23034–23045.
[21] W. Choi, M.G. Shin, C.H. Yoo, H. Park, Y.-I. Park, J.S. Lee, J.-H. Lee, Desalination membranes with ultralow biofouling via synergistic chemical and topological strategies, J. Membr. Sci., 626 (2021) 119212.
[22] C.H. Yoo, Y. Jo, J.H. Shin, S. Jung, J.-G. Na, T. Kang, J.S. Lee, Hierarchical membrane integration of shear stress-resistant nanoparticles and biomimetic micropatterns for ultrahigh and durable biofouling resistance, Chem. Eng. J., 432 (2022) 134363.
[23] K. Bachosz, M.T. Vu, L.D. Nghiem, J. Zdarta, L.N. Nguyen, T. Jesionowski, Enzyme-based control of membrane biofouling for water and wastewater purification: A comprehensive review, Environ. Technol. Innovation, 25 (2022) 102106.
[24] Y. Guo, C. Liu, H. Liu, J. Zhang, H. Li, C. Zhang, Contemporary antibiofouling modifications ofreverse osmosis membranes: State-of-the-art insights on mechanisms and strategies, Chem. Eng. J., 429 (2022) 132400.
[25] M.R. Parsek, E.P. Greenberg, Sociomicrobiology: the connections between quorum sensing and biofilms, Trends Microbiol., 13 (2005) 27–33.
[26] K.M. Smith, Y. Bu, H. Suga, Induction and inhibition of Pseudomonas aeruginosa quorum sensing by synthetic autoinducer analogs, Chem Biol, 10 (2003) 81-89.
[27] T.B. Rasmussen, M. Givskov, Quorum-sensing inhibitors as anti-pathogenic drugs, Int J Med Microbiol, 296 (2006) 149-161.
[28] T. Persson, T.H. Hansen, T.B. Rasmussen, M.E. Skinderso, M. Givskov, J. Nielsen, Rational design and synthesis of new quorum-sensing inhibitors derived from acylated homoserine lactones and natural products from garlic, Org Biomol Chem, 3 (2005) 253-262.
[29] M. Manefield, R. de Nys, K. Naresh, R. Roger, M. Givskov, S. Peter, S. Kjelleberg, Evidence that halogenated furanones from Delisea pulchra inhibit acylated homoserine lactone (AHL)-mediated gene expression by displacing the AHL signal from its receptor protein, Microbiology, 145 (1999) 283-291.
[30] S. Asghar, I.U. Khan, S. Salman, S.H. Khalid, R. Ashfaq, T.F. Vandamme, Plant-derived nanotherapeutic systems to counter the overgrowing threat of resistant microbes and biofilms, Adv. Drug Delivery Rev., 179 (2021) 114019.
[31] J.H. Choo, Y. Rukayadi, J.K. Hwang, Inhibition of bacterial quorum sensing by vanilla extract, Letters in Applied Microbiology, 42 (2006) 637-641.
[32] K. Ponnusamy, D. Paul, K. JiHyang, Inhibition of quorum sensing mechanism and Aeromonas hydrophila biofilm formation by Vanillin, Environmental Engineering Science, 26 (2009) 1359-1363.
[33] N. Mok, S.Y. Chan, S.Y. Liu, S.L. Chua, Vanillin inhibits PqsR-mediated virulence in Pseudomonas aeruginosa, Food Funct., 11 (2020) 6496–6508.
[34] S.-J. Choi, D.-K. Park, D. Jang, Y.-M. Yun, S. Kang, Changes of functional microbial genes by quorum sensing inhibition during the operation of forward osmosis, Environmental Engineering Research, 26 (2021) 190509-190500.
[35] S. Sharma, R. Pal, S. Hameed, Z. Fatima, Antimycobacterial mechanism of vanillin involves disruption of cell-surface integrity, virulence attributes, and iron homeostasis, International Journal of Mycobacteriology, 5 (2016) 460–468.
[36] D.J. Fitzgerald, M. Stratford, M.J. Gasson, J. Ueckert, A. Bos, A. Narbad, Mode of antimicrobial action of vanillin against Escherichia coli, Lactobacillus plantarum and Listeria innocua, Journal of Applied Microbiology, 97 (2004) 104-113.
[37] X. Si, X. Quan, Prevention of multi-species wastewater biofilm formation using vanillin and EPS disruptors through non-microbicidal mechanisms, International Biodeterioration & Biodegradation, 116 (2017) 211-218.
[38] V. Thiel, B. Kunze, P. Verma, I. Wagner-Döbler, S. Schulz, New structural variants of homoserine lactones in bacteria, ChemBioChem, 10 (2009) 1861-1868.

[39] L. Katebian, E. Gomez, L. Skillman, D. Li, G. Ho, S.C. Jiang, Inhibiting quorum sensing pathways to mitigate seawater desalination RO membrane biofouling, Desalination, 393 (2016) 135-143.
[40] A. Nam, J. Kweon, J. Ryu, H. Lade, C. Lee, Reduction of biofouling using vanillin as a quorum sensing inhibitory agent in membrane bioreactors for wastewater treatment, Membrane Water Treatment, 6 (2015) 189-203.
[41] S. Kappachery, D. Paul, J. Yoon, J.H. Kweon, Vanillin, a potential agent to prevent biofouling of reverse osmosis membrane, Biofouling, 26 (2010) 667-672.
[42] M. Esmaeili, T. Virtanen, J. Lahti, M. Mänttäri, M. Kallioinen, Vanillin as an Antifouling and Hydrophilicity Promoter Agent in Surface Modification of Polyethersulfone Membrane, Membranes (Basel), 9 (2019) 56.
[43] H. Shin, C. Park, C.-K. Lee, Y.-S. Lee, J.-O. Kim, Mitigating biofouling with a vanillin coating on thin film composite reverse osmosis membranes, Environmental Science and Pollution Research, 27 (2020) 1677-1685.
[44] L. Katebian, M.R. Hoffmann, S.C. Jiang, Incorporation of Quorum Sensing Inhibitors onto Reverse Osmosis Membranes for Biofouling Prevention in Seawater Desalination, Environmental Engineering Science, 35 (2018) 261-269.
[45] S.R. Kumar, G. Arthanareeswaran, Y. Lukka Thuyavan, A.F. Ismail, Enhancement of permeability and antibiofouling properties of polyethersulfone (PES) membrane through incorporation of quorum sensing inhibition (QSI) compound, Journal of the Taiwan Institute of Chemical Engineers, 72 (2017) 200-212.
[46] T. Virtanen, P. Parkkila, A. Koivuniemi, J. Lahti, T. Viitala, M. Kallioinen, M. Mänttäri, A. Bunker, Characterization of membrane–foulant interactions with novel combination of Raman spectroscopy, surface plasmon resonance and molecular dynamics simulation, Separation and Purification Technology, 205 (2018) 263-272.
[47] T. Virtanen, S.-P. Reinikainen, M. Kögler, M. Mänttäri, T. Viitala, M. Kallioinen, Real-time fouling monitoring with Raman spectroscopy, Journal of Membrane Science, 525 (2017) 312-319.
[48] L. Benavente, C. Coetsier, A. Venault, Y. Chang, C. Causserand, P. Bacchin, P. Aimar, FTIR mapping as a simple and powerful approach to study membrane coating and fouling, Journal of Membrane Science, 520 (2016) 477-489.
[49] V. Balachandran, K. Parimala, Vanillin and isovanillin: Comparative vibrational spectroscopic studies, conformational stability and NLO properties by density functional theory calculations, Spectrochim. Acta, Part A, 95 (2012) 354–368.
[50] C.E. Merzougui, Interactions des protéines sanguines avec interfaces polymères modifiées. Accessed: Feb. 07, 2022. Available: http://thesesups.ups-tlse.fr/5208/, in, PhD Thesis. Université Toulouse III - Paul Sabatier, France, 2021.
[51] J.L. Hutter, J. Bechhoefer, Calibration of atomic-force microscope tips, Review of Scientific Instruments, 64 (1993) 1868-1873.
[52] J. Chang, X. He, X. Bai, C. Yuan, The impact of hydrodynamic shear force on adhesion morphology and biofilm conformation of Bacillus sp, Ocean Eng., 197 (2020) 106860.
[53] D.R. Korber, J.R. Lawrence, L. Zhang, D.E. Caldwell, Effect of gravity on bacterial deposition and orientation in laminar flow environments, Biofouling, 2 (1990) 335-350.
[54] C. Voegel, A. Bertron, B. Erable, Biodeterioration of cementitious materials in biogas digester, Matériaux & Techniques, 2013 (2015).
[55] A. Beaussart, S. El-Kirat-Chatel, R.M.A. Sullan, D. Alsteens, P. Herman, S. Derclaye, Y.F. Dufrêne, Quantifying the forces guiding microbial cell adhesion using single-cell force spectroscopy, Nature Protocols, 9 (2014) 1049-1055.
[56] I. Demir, I. Lüchtefeld, C. Lemen, E. Dague, P. Guiraud, T. Zambelli, C. Formosa-Dague, Probing the interactions between air bubbles and (bio)interfaces at the nanoscale using FluidFM technology, J. Colloid Interface Sci., 604 (2021) 785–797.

[57] J. Geens, K. Boussu, C. Vandecasteele, B. Van der Bruggen, Modelling of solute transport in non-aqueous nanofiltration, J. Membr. Sci., 281 (2006) 139–148.
[58] D.G. Davies, M.R. Parsek, J.P. Pearson, B.H. Iglewski, J.W. Costerton, E.P. Greenberg, The Involvement of Cell-to-Cell Signals in the Development of a Bacterial Biofilm, Science, 280 (1998) 295-298.
[59] E. Dague, D. Alsteens, J.-P. Latgé, C. Verbelen, D. Raze, A.R. Baulard, Y.F. Dufrêne, Chemical Force Microscopy of Single Live Cells, Nano Lett., 7 (2007) 3026–3030.
[60] I. Demir, J. Blockx, E. Dague, P. Guiraud, W. Thielemans, K. Muylaert, C. Formosa-Dague, Nanoscale Evidence Unravels Microalgae Flocculation Mechanism Induced by Chitosan, ACS Appl. Bio Mater., 3 (2020) 8446–8459.
[61] M.D. Hoffman, L.I. Zucker, P.J.B. Brown, D.T. Kysela, Y.V. Brun, S.C. Jacobson, Timescales and Frequencies of Reversible and Irreversible Adhesion Events of Single Bacterial Cells, Anal. Chem., 87 (2015) 12032–12039.
[62] V. Carniello, B.W. Peterson, H.C. van der Mei, H.J. Busscher, Physico-chemistry from initial bacterial adhesion to surface-programmed biofilm growth, Adv. Colloid Interface Sci., 261 (2018) 1–14.
[63] S. Klemm, M. Baum, H. Qiu, Z. Nan, M. Cavalheiro, M.C. Teixeira, C. Tendero, A. Gapeeva, R. Adelung, E. Dague, M. Castelain, C. Formosa-Dague, Development of Polythiourethane/ZnO-Based Anti-Fouling Materials and Evaluation of the Adhesion of Staphylococcus aureus and Candida glabrata Using Single-Cell Force Spectroscopy, Nanomaterials, 11 (2021) 271.
[64] R. Bos, H.C. van der Mei, H.J. Busscher, Physico-chemistry of initial microbial adhesive interactions – its mechanisms and methods for study, FEMS Microbiol. Rev., 23 (1999) 179–230.
[65] S. Sharma, Y.A. Jaimes-Lizcano, R.B. McLay, P.C. Cirino, J.C. Conrad, Subnanometric Roughness Affects the Deposition and Mobile Adhesion of Escherichia coli on Silanized Glass Surfaces, Langmuir, 32 (2016) 5422-5433.
[66] C. Yao, T.J. Webster, M. Hedrick, Decreased bacteria density on nanostructured polyurethane, Journal of Biomedical Materials Research Part A, 102 (2014) 1823-1828.
[67] D. Breite, M. Went, I. Thomas, A. Prager, A. Schulze, Particle adsorption on a polyether sulfone membrane: how electrostatic interactions dominate membrane fouling, RSC Advances, 6 (2016) 65383-65391.
[68] H. Cai, H. Fan, L. Zhao, H. Hong, L. Shen, Y. He, H. Lin, J. Chen, Effects of surface charge on interfacial interactions related to membrane fouling in a submerged membrane bioreactor based on thermodynamic analysis, J. Colloid Interface Sci., 465 (2016) 33–41.
[69] E. Maikranz, C. Spengler, N. Thewes, A. Thewes, F. Nolle, P. Jung, M. Bischoff, L. Santen, K. Jacobs, Different binding mechanisms of Staphylococcus aureus to hydrophobic and hydrophilic surfaces, Nanoscale, 12 (2020) 19267–19275.
[70] K. Brindhadevi, F. LewisOscar, E. Mylonakis, S. Shanmugam, T.N. Verma, A. Pugazhendhi, Biofilm and Quorum sensing mediated pathogenicity in Pseudomonas aeruginosa, Process Biochemistry, 96 (2020) 49-57.
[71] G.M. Bruinsma, M. Rustema-Abbing, H.C. van der Mei, H.J. Busscher, Effects of cell surface damage on surface properties and adhesion of Pseudomonas aeruginosa, J. Microbiol. Methods, 45 (2001) 95–101.
[72] M. Crouzet, S. Claverol, A.-M. Lomenech, C. Le Sénéchal, P. Costaglioli, C. Barthe, B. Garbay, M. Bonneu, S. Vilain, Pseudomonas aeruginosa cells attached to a surface display a typical proteome early as 20 minutes of incubation, PLOS ONE, 12 (2017) e0180341.
[73] C.-Y. Chang, Surface Sensing for Biofilm Formation in Pseudomonas aeruginosa, Frontiers in Microbiology, 8 (2018).
[74] H. Salmi-Mani, G. Terreros, N. Barroca-Aubry, C. Aymes-Chodur, C. Regeard, P. Roger, Poly(ethylene terephthalate) films modified by UV-induced surface graft polymerization of vanillin derived monomer for antibacterial activity, European Polymer Journal, 103 (2018) 51-58.

[75] J. Azeredo, N.F. Azevedo, R. Briandet, N. Cerca, T. Coenye, A.R. Costa, M. Desvaux, G. Di Bonaventura, M. Hébraud, Z. Jaglic, M. Kačániová, S. Knøchel, A. Lourenço, F. Mergulhão, R.L. Meyer, G. Nychas, M. Simões, O. Tresse, C. Sternberg, Critical review on biofilm methods, Critical Reviews in Microbiology, 43 (2017) 313-351.
[76] A. Park, H.-H. Jeong, J. Lee, K.P. Kim, C.-S. Lee, Effect of shear stress on the formation of bacterial biofilm in a microfluidic channel, BioChip Journal, 5 (2011) 236.
[77] C. Lee, K., J. De Anda, A.E. Baker, R.R. Bennett, Y. Luo, E.Y. Lee, J.A. Keefe, J.S. Helali, J. Ma, K. Zhao, R. Golestanian, G.A. O'Toole, G.C.L. Wong, Multigenerational memory and adaptive adhesion in early bacterial biofilm communities, Proc. Natl. Acad. Sci. U.S.A., 115 (2018) 4471–4476.
[78] T.R. De Kievit, Quorum sensing in Pseudomonas aeruginosa biofilms, Environ. Microbiol., 11 (2009) 279–288.
[79] M.R. Parsek, E. Peter Greenberg, Quorum sensing signals in development of Pseudomonas aeruginosa biofilms, in: Methods in Enzymology, Academic Press, Cambridge, MA, USA, 1999, pp. 43–55.
[80] G.A. O'Toole, G.C.L. Wong, Sensational biofilms: surface sensing in bacteria, Curr. Opin. Microbiol., 30 (2016) 139–146.